Leonardo FLÓREZ-VALENCIA [1,2]**, Johan MONTAGNAT** [1]**, Maciej ORKISZ** [1]
[1] CREATIS, CNRS Research Unit (UMR 5515) affiliated to INSERM, Lyon, France,
[2] Universidad de los Andes, Bogotá, Colombia
{florez, montagnat, orkisz}@creatis.insa-lyon.fr

3D GRAPHICAL MODELS FOR VASCULAR-STENT POSE SIMULATION

Abstract

Stents are playing an increasing role in treatment of arterial stenoses and aneurysms. The goal of this work is to help the clinician in the pre-operative choice of the stent's length and diameter. This is done by "plunging" a model of the stent into real vascular 3D image. Two models are used. First, a simple geometrical model, composed of a set of circles or polygons stacked along the vessel's centerline, is used to simulate the introduction and the deployment of the stent. Second, a simplex-mesh model with an adapted cylindrical constraint is used to represent the stent surface. Another axially constrained simplex-mesh deformable model is used to reconstruct the 3D vessel wall. We simulate the interaction between the vessel wall and the stent by imposing that the model of the vessel locally fits the shape of the deployed-stent model. Preliminary quantitative results of the vessel reconstruction accuracy are given.

keywords: *vascular pathology, stenosis, stent, 3D image, simulation, generalized cylinder, simplex mesh, deformable model*

1 INTRODUCTION

Arterial-wall diseases, namely stenosis and aneurysm, belong to main causes of death in western countries. Aneurysm is a local distension of the artery (fig. 1 left), its rupture can lead to hemorrhage and stroke. Stenosis is an arterial lumen stricture (fig. 1 right), due to atherosclerotic plaque, which can lead to hypoperfusion, ischemia and infarct of organs that the artery irrigates. An increasing number of patients with these pathologies undergo an implantation of an endovascular prosthesis or of a stent. Stents are tubular grids that are deployed within stenotic regions in order to push the vascular wall outwards and thus keep open passageway for

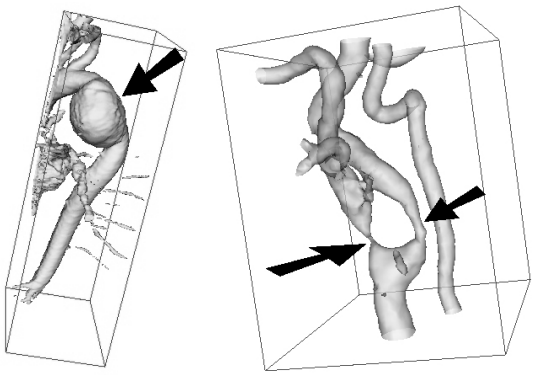

Fig. 1. Shaded-surface display of contrast-enhanced MRA images: aorta arch with an aneurysm (left), carotid artery with severe stenoses. Pathologies are indicated by arrows.

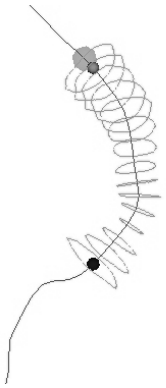

Fig. 2. Stenosed carotid artery from fig. 1 segmented by Maracas software: vessel centerline and stacking of contours orthogonal to this line.

blood flow. Endo-prostheses are similar to stents, but covered with a blood-proof tissue. Implanted within an aneurysm, an endo-prosthesis canalizes the blood flow and reduces pressure on the arterial wall, thus preventing rupture. When folded, stents and endo-prostheses are slim and can be inserted into the artery, using a catheter. Deployed by shape-memory effect or by an inflating balloon, they become shorter and should fit the diameter of the artery's healthy part. Appropriate pre-operative choice of stent (endo-prosthesis) dimensions is necessary to avoid loosening, thrombus formation, embolism and branching-vessel obstruction.

The goal of our work is to aid this choice by providing a simulation tool able to represent stent-deployment within the given patient's artery. For the sake of conciseness, "stent" will be used in the sequel to denote both stents and endo-prostheses.

Several recent studies aim at extracting patients' individual vascular 3D geometry and/or at simulating radiological vascular interventions. Virtual vascular project [1] [17] concentrates on the simulation of insertion of surgical needles and of catheters. In MedIS-VR project virtual endoscopic viewing is used for preoperative aortic stent planning. The vessel centerline is first automatically extracted. A virtual stent is then placed along this path. Its length and its diameters are finally interactively adjusted [11]. Another project, named Geodesic, brings together automatic and semi-automatic segmentation tools and combines them with mesh generation tools in order to build patient-specific vascular models [15]. These models are then used for surgical planning, *e.g.* simulation of revascularization, flow simulation, etc. A similar approach has been followed by the authors of simulation-based medical planning software ASPIRE [12][13]. In [2], the patient-specific vascular geometry is automatically segmented using a tubular deformable mesh model [16]. The stent model is also a cylindrical mesh. Merging both meshes simulates artery stenting.

In our work, we follow a similar approach. However, instead of mesh merging, we attempt to simulate stent/vascular-wall interaction. The vascular lumen 3D image is first acquired using contrast-enhanced magnetic resonance angiography (MRA) technique [4]. This image is then segmented (fig. 2) using Maracas, a software developped in our laboratory [7]. The segmentation method is based on generalized-cylinder model and provides the axial shape of the vessel, planar contours orthogonal to the vessel centerline and estimated values of local vascular lumen radii [6]. Simulation of stent insertion and deployment is carried out using a simplified geomet-

rical model "pulled on" the centerline. This model is described in section 2. A more realistic representation of the stent and of the vessel wall surface, as well as interaction between them, is then realized using simplex-mesh deformable model presented in section 3.

2 GEOMETRICAL MODEL

A generalized cylinder, as used in Maracas for vessels representation, *i.e.* a stacking of contours orthogonal to the centerline, can also be used to model stents. Let $A_p(l_p)$ and $A_v(l_v)$ be parametric 3D curves representing the centerlines of the stent and of the vessel respectively, with $l_p \in [0,1]$ and $l_v \in [0,1]$ the arc-length parameters. The discretized version of each centerline $A(l)$ is a set of vertices $\{\mathbf{a}_i\}$. The discretization of $A_v(l_v)$ is not uniform, while $A_p(l_p)$ has to be uniformly discretized. The absolute length of the vascular segment L_v provided by Maracas is greater than the maximum length L_{pM} of the stent. Let furthermore $C_p(l_p)$ be a planar contour orthogonal to $A_p(l_p)$ and centered at the centerline point corresponding to the arc-length l_p.

The initial model of the stent is constructed by placing predefined-shape contours $C_p(l_p)$, cirular or polygonal, equally spaced along a straight axis. It is assumed that the stent does not modify the vessel's axial shape. This implicitly means that the stent is much more flexible than the vessel wall. Fitting the stent to the vessel axial shape can then be seen as a process of sliding the predefined shape $C_p(l_p)$ along the centerline $A_v(l_v)$, while keeping the contour plane orthogonal to this line (fig. 3). This is obtained by mapping the axis $A_p(l_p)$ of the initial straight model of the stent onto the vessel centerline $A_v(l_v)$. The stent model is placed between l_{v0} and an end point at l_{vM}, with l_{v0} a user-defined delivery point and l_{vM} an end point automatically deduced (for a given radius) from the length/radius relation that characterizes the stent-expansion process [5].

This geometrical model is very useful to simulate the stent displacement along the vessel centerline and to interact with the user in order to choose the delivery region and the stent parameters. Once deployed, this model provides the exact length and location of the stent. However, the surface thus constructed is not regular. Contours orthogonal to the centerline may intersect each other, where the centerline is curved (fig. 4 middle). The surface is difficult to represent and appears locally folded. Furthermore, this model is not well-suited for the simulation of stent/vessel-wall interaction. Another model, based on a simplex mesh, is therefore used to simulate this interaction and to display the final result. This model is constrained by the centerline segment $A_v(l_v)$, $l_v \in [l_{v0}, l_{vM}]$.

3 SIMPLEX MODEL

Simplex meshes are discrete representations of surfaces suited to deformation [3]. In 2-simplex meshes used to represent surfaces, each vertex has exactly three neighbors. 2-simplex meshes are topologically dual to triangulations, thus making conversions back and forth easy. In this work, we propose a specific constraint of the simplex meshes deformation framework [9] adapted to cylindrical shape deformation [8].

3.1 Model deformation

A simplex surface is represented by a set of vertices $\{\mathbf{v}_i\}$. For deformation purposes, each vertex undergoes a deformation controlled by an internal (regularizing) energy term and an external (data-driven) term. Discretization of the energy minimization framework leads to the evolutive equation:

$$\mathbf{v}_i^{t+1} = \mathbf{v}_i^t + \gamma(\mathbf{v}_i^t - \mathbf{v}_i^{t-1}) + \mathbf{f}_i^{\text{int}} + \beta\mathbf{f}_i^{\text{ext}} \quad (1)$$

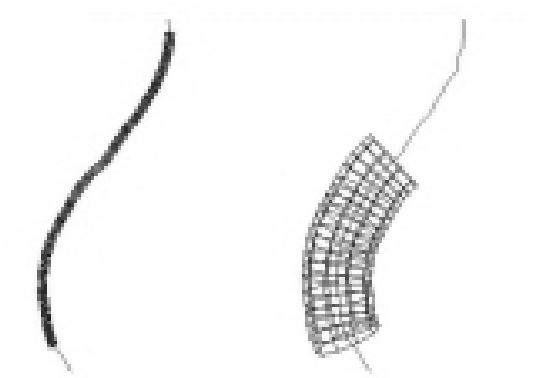

Fig. 3. Simulation of stent insertion and deployment using a simplified geometrical model: a contracted stent is placed along a catheter and guided until the delivery location (left), once expanded the stent becomes shorter (right).

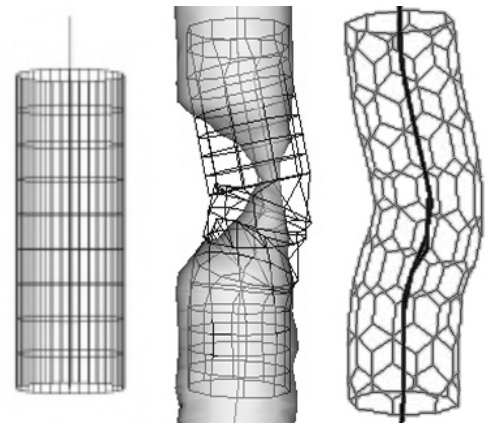

Fig. 4. Stent representation in a straight (left) and curved-centerline region: the geometrical model generates an irregular folded surface due to intersections of contours (middle), a simplex-mesh model generates a regular surface (right).

where $\mathbf{v}_i^t$ denotes the location of vertex $\mathbf{v}_i$ at iteration t, $\beta \in [0, 1]$ is the external force weight, and γ is a damping parameter. The discretization time step is hidden in the weighting coefficients. The computation of the internal force $\mathbf{f}_i^{\text{int}}$ is specific to the simplex mesh geometry and enforces regularity of the shape curvature (see [9, 3] for details). The external force ensures an attraction of the model towards the vessel boundary in the image. Both forces are computed as displacement vectors along the simplex-surface normal. Location of the vascular-lumen boundary depends on image acquisition modality. Hence, this force is also modality-dependent and uses either gradient intensity or an iso-value dependent on the maximum intraluminal signal. An empirical study on contrast-enhanced MRA images of vessel-phantoms with stenoses has shown that the real boundary does not correspond to gradient maximum but rather to 45% of the local intra-luminal maximum of intensity. This iso-value is therefore used for the computation of the external forces.

3.2 Model extension to generalized cylinders

Equation 1 defines the local deformation of each surface vertex but it does not take into account the particular shape and expected properties of the modeled object. When dealing with vessels, one expects cylindrical structures with a high bending capability but for which deformations should preserve the generalized cylinder shape (fig. 4 right and fig. 5 left). Biomechanical models [10] are suited for that kind of physical deformations but they are very costly. Instead, we propose an extension of our surface model.

The surface is bound to the centerline: each surface vertex $\mathbf{v}_j$ is associated with the 3 closest centerline vertices $\{\mathbf{a}_{i-1}, \mathbf{a}_i, \mathbf{a}_{i+1}\}$ (fig. 5 right). Conversely, we denote $\mathcal{E}_i$ the set of surface vertices bound to the centerline vertex $\mathbf{a}_i$. Each pair of vertices $(\mathbf{a}_i, \mathbf{v}_j)$ is weighted by a coefficient ν_{ij} such that $\sum_j \nu_{ij} = 1$. When the model surface undergoes some deformation,

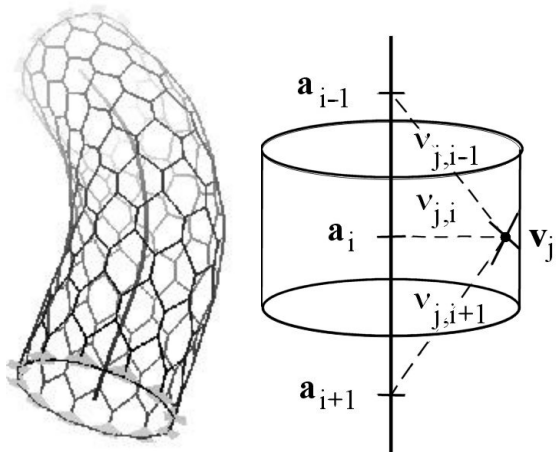

Fig. 5. Deformed cylinder (left) and notations diagram (right)

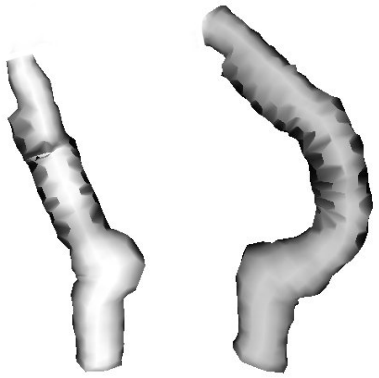

Fig. 6. Simulation of stent/vessel-wall interaction in real stenosed carotid arteries from (fig. 1). Each vessel of interest is displayed separately.

the centerline bends accordingly through an external force resulting from the surface forces:

$$\mathbf{f}^{\text{ext}}(\mathbf{a}_i) = \frac{\sum_{\mathbf{v_j} \in \mathcal{E}_i} \nu_{ij} \mathbf{f}^{\text{ext}}(\mathbf{v}_j)}{\sum_{\mathbf{v_j} \in \mathcal{E}_i} \nu_{ij}} \tag{2}$$

The centerline is considered as a 1-simplex mesh in $I\!R^3$ and the external force (2) is used to compute its deformation. Conversely, the centerline bending is reported to the surface as the sum of an axial component (each vertex tends to follow the axis global motion) and a radial component (each vertex tends to align on a circle around the centerline) with:

$$\begin{array}{l} \mathbf{f}^{\text{axial}}(\mathbf{v}_j) = \sum_{k=i-1}^{k=i+1} \nu_{kj} \mathbf{f}(\mathbf{a}_k) \\ \mathbf{f}^{\text{radial}}(\mathbf{v}_j) = \sum_{k=i-1}^{k=i+1} \mathbf{v}_j^{\perp} + \left((1-\xi)\|\mathbf{v}_j^{\perp}\mathbf{v}_j\| + \xi r_k\right) \mathbf{n}_j - \mathbf{v}_j \end{array} \tag{3}$$

where $\mathbf{v}_j^{\perp}$ is the orthogonal projection of $\mathbf{v}_j$ onto the centerline, $\mathbf{n}_j$ is the unit normal vector of the centerline in $\mathbf{v}_j^{\perp}$, r_k is the radius (mean distance of the surface vertices to the centerline) in $\mathbf{a}_k$ and ξ is a radial weight. The surface vertices are thus submitted to the internal and external forces (local forces) plus the axial and radial forces (centerline forces). Let $\lambda \in [0,1]$ weight the contributions of the local and centerline forces. The equation 1 becomes:

$$\mathbf{v}_i^{t+1} = \mathbf{v}_i^t + \gamma(\mathbf{v}_i^t - \mathbf{v}_i^{t-1}) + \lambda\left(\mathbf{f}_i^{\text{int}} + \beta \mathbf{f}_i^{\text{ext}}\right) + (1-\lambda)\left(\mathbf{f}^{\text{axial}}(\mathbf{v}_i^t) + \mathbf{f}^{\text{radial}}(\mathbf{v}_i^t)\right) \tag{4}$$

3.3 Model initialization

Deformable models are sensitive to their initialization as they usually converge towards a local minimum of their energy functional. In our application however, Maracas accurately extracts centerline points $\{\mathbf{a}_i\}$ and roughly estimates a set of radii $\{r_i\}$. This provides an initialization of the simplex-mesh model close to the vessel boundary and, together with the axial constraint, can be successfully used for 3D segmentation of the vessel. However, the model of the vessel-lumen surface has to interact with a model of the stent in order to converge towards a realistic representation of the stented vessel.

3.4 Stent modeling

Stent-deployment simulation using the simplified geometrical model described in the section 2, provides the stent-axis mapping onto the vessel centerline calculated by Maracas, between the bounds l_{v0} and l_{vM}, for a given stent radius r. The stent surface is represented using a new cylindrical simplex model combining the mapped centerline and the radius r. Once constructed, this model remains static, *i.e.* it is not submitted to deformations. In the stent area (between l_{v0} and l_{vM}), the shape of the vessel-surface model is controlled by the stent shape rather than the external forces extracted from the image data. Therefore, the external force of the vessel-surface model is locally set to zero. Instead, the corresponding section of the vessel-surface model is attracted by the surface of the stent model.

4 RESULTS AND CONCLUSION

The above described procedure was applied to simulate stent introduction and expansion in real arteries (fig. 6) and in six phantoms (fig. 7). Visualisation of a virtual stent deployed in real MRA data volume is useful for preoperative assessment of the stent's diameter and length. Simulation of the interaction between the vascular wall and the stent generates a realistic view of the luminal shape modification induced by the stent. The simplex-mesh deformable model used for this simulation is applicable to vascular-image segmentation and quantification (fig. 7). Average error of stenosis quantification in the images of phantoms was 7.3%. The largest errors occurred in complex stenoses, where the shape was no more cylindrical, and in 95% stenoses due to the lack of signal.

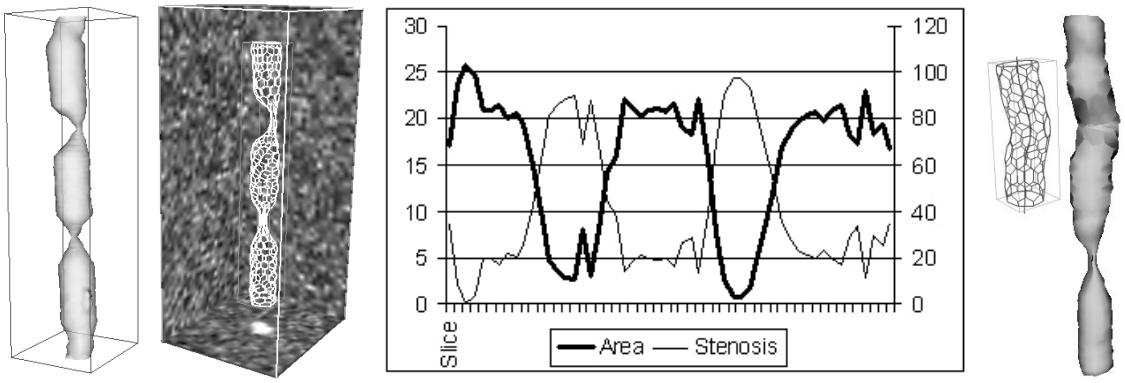

Fig. 7. Simulation of stent/vessel-wall interaction in a physical phantom of stenosed vessel. From left to right: shaded-surface display of an MRA image of the phantom, simplex mesh resulting from its segmentation and "plunged" into the original image, quantification curves, deformed stent model, and shaded-surface display of the vessel with the stent inside.

Our simulation is based on the simplifying assumption that the stent does not modify the axial geometry of the vessel. However, it has been demonstrated [14] that the stent may locally change the vessel's curvature. As the stent tends to locally stiffen the vessel, the latter may be stretched outside the stented section, thus modifying its actual dimensions. Axial stiffness can be included in our deformable model, in order to simulate this phenomenon. However, this improvement of the model is not straightforward. The link between the weighting coefficient of the stiffness force and the physical properties of the vessels is not obvious. Furthermore, these

properties are locally modified by the presence of atherosclerotic plaque that is more or less rigid depending on its composition. Moreover, the vessels within the body are not free, their shape strongly depends on the influence of the surrounding tissues. These open questions leave a wide field for further research combining biomechanical modelling and multi-modality image processing including high-resolution MR, computed tomography and intravascular ultrasound.

5 ACKNOWLEDGEMENTS

This work has been supported by Rhone-Alpes Region project ADeMo. It falls within the scope of scientific topics of GdR PRC ISIS. The authors are grateful to Professor Philippe C. Douek for providing MRA images.

REFERENCES

[1] ABDOULAEV, G., CADEDDU, S., DELUSSU, G., DONIZELLI, M., FROMAGGIA, L., GIANCHETTI, A., GOBBETTI, E., LEONE, A., MANZI, C., PILI, P., SCHEININE, A., TUVERI, M., VARONE, A., VENEZIANI, A., ZANETTI, G., AND ZORCOLO, A. Viva: The virtual vascular project. *IEEE Transactions on Information Technology in Biomedicine 22*, 4 (1998).

[2] CEBRAL, J. R., LOHNER, R., SOTO, O., CHOYKE, P. L., AND YIM, P. J. Patient-specific simulation of carotid artery stenting using computational fluid dynamics. In *Medical Image Computer and Computer Assisted Intervention (MICCAI)* (Utrecht, The Netherlands, 2001), pp. 153–160.

[3] DELINGETTE, H. General Object Reconstruction based on Simplex Meshes. *International Journal of Computer Vision 32*, 2 (1999), 111–146.

[4] DOUEK, P. C., REVEL, D., CHAZEL, S., FALISE, B., VILLARD, J., AND AMIEL, M. Fast mr angiography of the aortoiliac arteries and arteries of the lower extremity: value of bolus-enhanced, whole-volume subtraction technique. *American Journal of Radiology*, 165 (1995), 431–437.

[5] DUMOULIN, C., AND COCHELIN, B. Mechanical behaviour modelling of balloon-expandable stents. *Journal of Biomechanics 33* (2000), 1461–1470.

[6] HERNANDEZ-HOYOS, M., ANWANDER, A., ORKISZ, M., ROUX, J. P., DOUEK, P. C., AND MAGNIN, I. E. A Deformable Vessel Model with Single Point Initialization for Segmentation, Quantification and Visualization of Blood Vessels in 3D MRA. In *Medical Image Computer and Computer Assisted Intervention (MICCAI)* (Pittsburgh, PA, USA, Oct. 2000), pp. 735–745.

[7] HERNANDEZ-HOYOS, M., ORKISZ, M., PUECH, P., MANSARD-DESBLEDS, C., DOUEK, P. C., AND MAGNIN, I. E. Computer-assisted analysis of three-dimensional angiograms. *RadioGraphics 22* (2002), 421–436.

[8] MONTAGNAT, J., AND DELINGETTE, H. A Hybrid Framework for Surface Registration and Deformable Models. In *Proceedings of Computer Vision and Pattern Recognition (CVPR)* (San Juan, Puerto Rico, June 1997), pp. 1041–1046.

[9] MONTAGNAT, J., AND DELINGETTE, H. Globally constrained deformable models for 3D object reconstruction. *Signal Processing 71*, 2 (Dec. 1998), 173–186.

[10] PHAM, Q. C., VINCENT, F., CLARYSSE, P., CROISILLE, P., AND MAGNIN, I. E. A FEM-based deformable model for the 3D segmentation and tracking of the heart in cardiac MRI. In *International Symposium on Image and Signal Processing and Analysis* (Pula, Croatia, 2001), pp. 250–254.

[11] STERN, C., WILDERMUTH, S., WEISSMANN, J., STUCKI, P., HILFIKER, P., AND DEBATIN, J. Predictive medicine: Computational techniques in therapeutic decision-making. In *Computer Assisted Radiology and Surgery (CARS)* (Paris, France, 1999), pp. 176–180.

[12] TAYLOR, C., DRANEY, M., KU, J., PARKER, D., STEELE, B., WANG, K., AND ZARINS, C. Predictive medicine: Computational techniques in therapeutic decision-making. *Computer Aided Surgery*, 4 (1999), 231–247.

[13] WANG, K., DUTTON, R., AND TAYLOR, C. Improving geometric model construction for blood flow modeling. *IEEE Engineering in Medicine and Biology 18*, 6 (1999), 33–39.

[14] WENTZEL, J., WHELAN, D., GIESSEN, W. V. D., BEUSEKOM, H. V., ANDHYISWARA, I., SERRUYS, P., SLAGER, C., AND KRAMS, R. Coronary stent implantation changes 3D vessel geometry and 3D shear stress distribution. *Journal of Biomechanics 33* (2000), 1287–1295.

[15] WILSON, N., WANG, K., DUTTON, R. W., AND TAYLOR, C. A software framework for creating patient specific geometric models from medical imaging data for simulation based medical planning of vascular surgery. In *Medical Image Computer and Computer Assisted Intervention (MICCAI)* (Utrecht, The Netherlands, 2001), pp. 449–456.

[16] YIM, P. J., CEBRAL, J. R., MULLICK, R., MARCOS, H. B., AND CHOYKE, P. L. Vessel surface reconstruction with a tubular deformable model. *IEEE Transactions on Medical Imaging 20*, 10 (2001), 1411–1421.

[17] ZORCOLO, A., GOBBETTI, E., ZANETTI, G., AND TUVERI, M. A volumetric virtual environment for catheter insertion simulation. Center for Advanced Studies, Research and Development (CRS4) http://www.crs4.it.